



CDF note 7676

## Search for Neutral MSSM Higgs Bosons Decaying to Tau Pairs

The CDF Collaboration  
URL <http://www-cdf.fnal.gov>  
(Dated: August 26, 2005)

We present the results of a search for inclusive production of neutral MSSM Higgs bosons in  $p\bar{p}$  collisions at 1.96 TeV center of mass energy. The data were collected with the CDF II detector at the Tevatron collider at Fermilab, and correspond to an integrated luminosity of  $310 \text{ pb}^{-1}$ . The search is performed in the  $\text{di-}\tau$  Higgs decay mode. No significant excess of events above the standard model backgrounds is observed. The measurements are used to set exclusion limits on production cross-section times branching fraction to tau pairs for Higgs masses in the range from 90 to 250  $\text{GeV}/c^2$ .

*Preliminary Results for Summer 2005 Conferences*

## I. INTRODUCTION

One of the outstanding questions in modern particle physics is the dynamics of electroweak (EW) symmetry breaking and the origin of particle masses. In the standard model (SM), EW symmetry is spontaneously broken through the Higgs mechanism [1], by the introduction of a doublet of self-interacting complex scalar fields with non-zero vacuum expectation values. The physical manifestation of this scenario is the existence of a massive scalar Higgs boson  $h_{SM}$ . Theoretical difficulties related to divergent radiative corrections to the  $h_{SM}$  mass have natural solution in supersymmetric (SUSY) models.

The minimal supersymmetric extension of the standard model (MSSM) is the simplest realistic SUSY theory. It requires two Higgs doublets resulting in a Higgs sector with two charged and three neutral scalar bosons. Assuming  $CP$ -invariance, one of the neutral bosons ( $A$ ) is  $CP$ -odd, and the other two ( $h, H$ ) are  $CP$ -even. Throughout this Note we use  $h$  ( $H$ ) for the lighter (heavier)  $CP$ -even neutral Higgs boson, and  $\phi$  to denote any of  $h, H, A$ . At tree level, the MSSM Higgs bosons are described by two free parameters, chosen to be the mass of  $A$  ( $m_A$ ), and  $\tan\beta = v_2/v_1$ , where  $v_2, v_1$  are the vacuum expectation values of the neutral Higgs fields that couple to up-type and down-type fermions, respectively. The Yukawa couplings of  $A$  to down-type fermions (such as the  $b$  quark and  $\tau$ ) are enhanced by a factor of  $\tan\beta$  relative to the SM. For large  $\tan\beta$  one of the  $CP$ -even bosons is nearly mass-degenerate with  $A$  and has similar couplings.

There are two dominant production mechanisms of neutral MSSM Higgs bosons at hadronic colliders: gluon fusion [2] and  $b\bar{b}$  fusion [3, 4]. The leading decay modes of  $A$  and the corresponding mass-degenerate  $CP$ -even Higgs boson are  $\phi \rightarrow b\bar{b}$  ( $\sim 90\%$ ) and  $\phi \rightarrow \tau\tau$  ( $\sim 10\%$ ). Despite the smaller branching fractions, Higgs searches in the di- $\tau$  channel have advantages. They do not suffer from the large di-jet and multi-jet backgrounds as  $\phi \rightarrow b\bar{b}$ .

In this Note we present the results of a search for inclusive production of neutral MSSM Higgs bosons in  $p\bar{p}$  collisions at  $\sqrt{s}=1.96$  TeV. The search is performed in the  $\phi \rightarrow \tau\tau$  decay channel and uses data collected with the CDF detector in Run II of the Fermilab Tevatron. One of the  $\tau$ 's is detected in the leptonic, and the other one in the semi-hadronic decay modes. The analyzed data sample corresponds to an integrated luminosity of  $310 \text{ pb}^{-1}$ .

## II. THE CDF DETECTOR

CDF II is a general purpose detector built to study particles produced in  $p\bar{p}$  collisions at  $\sqrt{s}=1.96$  TeV. The following is a short overview of the systems relevant to this search.

The CDF II tracking system consists of a cylindrical wire drift chamber and silicon micro-strip detectors, coaxial with the  $p$  and  $\bar{p}$  beams. It is immersed in a 1.4 T uniform magnetic field produced by a superconducting solenoid. Electromagnetic (EM) and hadronic (HAD) sampling calorimeters are located outside the tracking system and cover pseudorapidity  $|\eta| < 3.6$ . They are divided into towers with projective geometry. A Shower Maximum Detector (CES) is embedded in the EM calorimeter at a depth of six radiation lengths. CES consists of proportional chambers with anode wires going parallel to the beam axis, and orthogonal cathode strips. CES is used to determine the position of electromagnetic showers with spatial resolution of  $\sim 0.5$  cm. Muons are identified by a system of drift chambers located outside the calorimeter volume. The combined coverage of the central muon detectors extends to  $|\eta| < 1.1$ . The luminosity is measured by gas Cherenkov counters located in the detector far forward and backward regions ( $3.7 < |\eta| < 4.7$ ) with 6% precision [5]. Detailed description of CDF II can be found in [6].

## III. DATA SAMPLE & EVENT SELECTION

The events in the analyzed data sample were selected with “lepton plus track” triggers [7]. They require a lepton ( $e, \mu$ ) candidate and an isolated track with transverse momentum  $p_T > 5$  GeV/c, both pointing to the central detector ( $|\eta| \lesssim 1$ ) and having azimuthal separation  $\Delta\varphi > 10^\circ$ . At trigger level, an electron is defined as a track with  $p_T > 8$  GeV/c matched to a cluster in CES, and a cluster in the EM calorimeter with transverse energy  $E_T > 8$  GeV. Tracks with  $p_T > 8$  GeV/c associated with hits in the muon detectors are identified as muon candidates. The overall trigger efficiency for signal selection is greater than 90%.

The detection of  $\phi \rightarrow \tau\tau$  requires identification of  $e, \mu$  (from leptonic  $\tau$  decays) and the reconstruction of the products of semi-hadronically decaying  $\tau$ 's. In the following, we use  $\tau_e, \tau_\mu,$  and  $\tau_{had}$  as short-hand notations for the

decay modes  $\tau \rightarrow e\nu_e\nu_\tau$ ,  $\tau \rightarrow \mu\nu_\mu\nu_\tau$ , and  $\tau \rightarrow \text{hadrons } \nu_\tau$ , respectively. In this notation, the investigated di- $\tau$  final states are  $\tau_e\tau_{had}$  and  $\tau_\mu\tau_{had}$ . The algorithms for  $e$  and  $\mu$  identification are described in detail in [6]. The sum of the transverse momenta of the neutrinos from  $\tau$  decays appears as missing transverse energy ( $\cancel{E}_T$ ). It is determined from the imbalance of energy deposition in the calorimeter in the transverse plane.  $\cancel{E}_T$  is corrected for the position of the interaction vertex and transverse momenta of identified muons.

The acceptances for signal and most of the backgrounds are determined from samples of Monte Carlo (MC) simulated events produced by the PYTHIA event generator [8] with CTEQ5L [9] parton distribution functions (PDF's). Tau decays are simulated by the TAUOLA package [10]. Detector response is simulated with a GEANT-based [11] model of the detector.

### A. Tau Reconstruction and Isolation

The decay products in  $\tau_{had}$  appear as narrow jets with low track and  $\pi^0$  multiplicity. We use a variable-size cone algorithm to associate these particles with  $\tau$  candidates. The positions of  $\pi^0$ 's are determined from hits in the CES detector, and the energy is measured by the EM calorimeter. A charged track with  $p_T > 6.0$  GeV/c pointing to a cluster of six or less contiguous towers serves as a "seed" for a tau candidate. The direction of the seed track defines the axis of a signal cone and an isolation annulus. The angular size of the signal cone  $\alpha_{sig}$  is a function of the calorimeter cluster energy  $E_{cl}$ . The isolation annulus extends from  $\alpha_{sig}$  to  $\alpha_{iso} = 30^\circ$ . The value of  $\alpha_{sig}$  is the minimum of  $10^\circ$  and  $(5 \text{ GeV})/E_{cl}$  rad. To prevent position resolution effects, the minimum value of  $\alpha_{sig}$  is set to 0.05 rad for tracks, and 0.1 rad for  $\pi^0$ 's. The four-momentum of  $\tau_{had}$  is calculated from tracks and  $\pi^0$ 's contained in the signal cone. Particles in the isolation annulus are used to impose isolation requirements that discriminate against quark and gluon jets: The sum of the transverse momenta of tracks (sum of transverse energy of  $\pi^0$ 's) in the isolation annulus is required to be less than 1 GeV/c (1 GeV). We select tau candidates with transverse momentum of the hadronic system  $p_T^{had} > 15$  GeV/c, and invariant mass  $m_{had} < 1.8$  GeV/c<sup>2</sup>. The number of tracks with  $p_T > 1$  GeV/c in the signal cone ( $N_{sig}^{trk}$ ) is restricted to one or three (consistent with the dominant  $\tau$  decay modes). In the  $N_{sig}^{trk} = 3$  case the sum of the electric charges must be equal to  $\pm 1$ . Electrons are rejected by imposing the condition  $(E_{cl}/P_{sig}^{trk})(0.95 - f) > 0.1$ ,  $f$  is the ratio of electromagnetic to hadronic energy in the cluster, and  $P_{sig}^{trk}$  is the scalar sum of track momenta in the signal cone.

Tau identification efficiency has a turn-on region between  $p_T^{had} = 15$  GeV/c and  $p_T^{had} = 25$  GeV/c, and reaches a plateau of  $\sim 46\%$ . The misidentification probability for a quark or gluon jet as  $\tau_{had}$  is  $\sim 1.5\%$  for jet transverse energy  $E_T^{jet} = 20$  GeV, falling down to  $\sim 0.1\%$  for  $E_T^{jet} = 100$  GeV.

### B. Backgrounds

The dominant (and irreducible) background in the final sample of selected events is from  $Z/\gamma^*$  production with subsequent decays to  $\tau$  pairs. It is estimated using MC simulated events with normalization corresponding to  $\sigma(p\bar{p} \rightarrow Z/\gamma^*) \times BR(Z/\gamma^* \rightarrow ll) = 254.9$  pb in the di-lepton mass region  $66 < m_{ll} < 116$  GeV/c<sup>2</sup> [12]. The second-largest contribution is from backgrounds involving gluon or quark jets misidentified as  $\tau_{had}$ , such as di-jet and multi-jet events,  $W$  produced in association with jets, and photon plus jet production. These backgrounds are estimated from the data by applying  $jet \rightarrow \tau$  misidentification rates to jets in events that pass all selection criteria except for  $\tau_{had}$  identification. The misidentification rates are obtained from independent jet samples, and verified using control regions corresponding to the discussed underlying processes. The third group of considered backgrounds includes  $Z$  ( $Z \rightarrow ee, \mu\mu$ ),  $WW$ ,  $WZ$ ,  $ZZ$ , and  $t\bar{t}$  production. They are determined from MC samples.

### C. Event Cuts

The events in the  $\tau_e\tau_{had}$  ( $\tau_\mu\tau_{had}$ ) channel are selected by requiring one  $e$  ( $\mu$ ) candidate with  $p_T^{e(\mu)} > 10$  GeV/c, and one hadronically decaying  $\tau$  candidate with  $p_T^{had} > 15$  GeV and opposite electric charge. Low-energy multi-jet backgrounds are suppressed by rejecting events with  $|p_T^{e(\mu)}| + |p_T^{had}| + |\cancel{E}_T| < 50$  GeV. Backgrounds from  $W + jet$

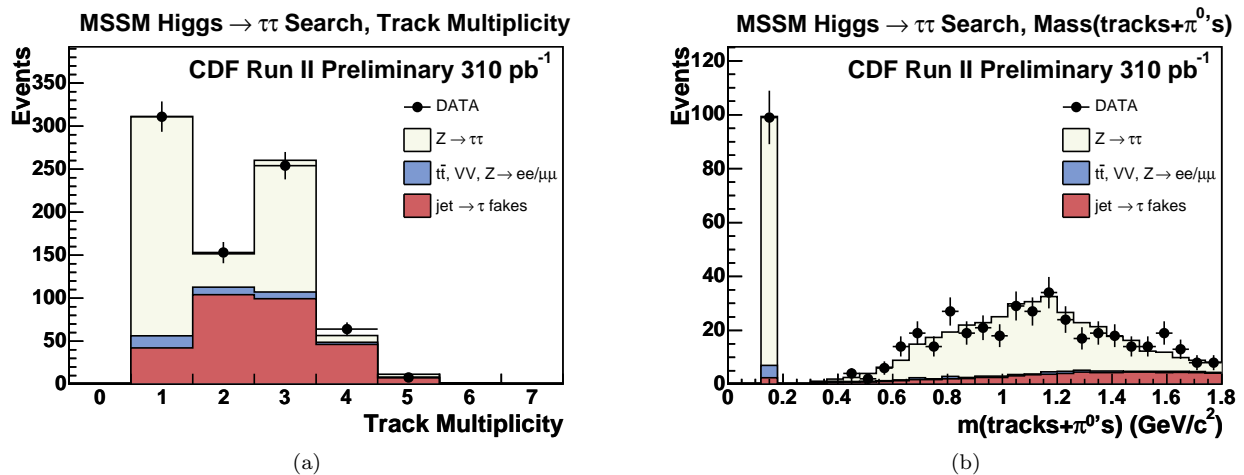


FIG. 1: Track multiplicity for hadronically decaying tau candidates before applying  $N_{trk}^{sig} = 1, 3$  and opposite charge requirements (a). Mass of the hadronic system (b) after all cuts are applied.

events (with  $W \rightarrow e(\mu)\nu$  and misidentified jet) are suppressed by imposing requirement on the relative directions of the visible tau decay products, and  $\cancel{E}_T$ . We define a bisection axis  $\zeta$  of the angle between the directions of  $e(\mu)$  and  $\tau_{had}$  in the transverse plane. The projections  $p_{\zeta}^{vis} = (\vec{p}_{e(\mu)} + \vec{p}_{had}) \cdot \hat{\zeta}$  and  $p_{\zeta}^{\cancel{E}_T} = \vec{\cancel{E}}_T \cdot \hat{\zeta}$  are required to satisfy  $p_{\zeta}^{\cancel{E}_T} > 0.6p_{\zeta}^{vis} - 10$  GeV/c. This condition removes  $\sim 85\%$  of the surviving  $W + \text{jet}$  events, while signal losses are  $< 5\%$ . To suppress backgrounds from  $Z \rightarrow ll$  decays with a misidentified lepton, we do not accept events with invariant mass of an  $e(\mu)$  and a single-track  $\tau_{had}$  candidate within 10 GeV/c $^2$  of the  $Z$  mass.

Figure 1a shows the track multiplicity distribution for hadronically decaying  $\tau$  candidates in the data, along with the background predictions. This plot is produced *before* applying the opposite charge, and  $N_{trk}^{sig}$  requirements discussed above. The characteristic enhancement in the one- and three-track bins demonstrates clear excess of events with  $\tau_{had}$  in the final state. The mass of the hadronic system after applying all  $\tau$  identification requirements is shown in Figure 1b. The total number of expected SM background events after applying all selection criteria is  $N_{bg}^{ev} = 496.1 \pm 5.4 \pm 27.7 \pm 24.8$ , where the first error is statistical, the second one is systematic, and the third one is the uncertainty in the measured integrated luminosity. The contributions from  $Z/\gamma^* \rightarrow \tau\tau$ , backgrounds with  $jet \rightarrow \tau$  misidentification, and all remaining background sources are 404.5, 75.4, and 16.5, respectively. The signal acceptance for a Higgs boson of mass 90 GeV/c $^2$  (250 GeV/c $^2$ ) is 0.8% (2.0%).

#### D. Systematic Uncertainties

The systematic uncertainties for particle identification efficiency are 3.5% ( $\tau_{had}$ ), 1.3% ( $e$ ), and 4.6% ( $\mu$ ). The uncertainties in trigger efficiency for the  $\tau_e\tau_{had}$  and  $\tau_\mu\tau_{had}$  channels are 2.1% and 1.4%, respectively. The uncertainty in the determination of backgrounds due to  $jet \rightarrow \tau$  misidentification is 20%, resulting in 3% effect on the total background estimate. The systematic uncertainty in signal acceptance from event-level cuts is less than 2%. The imprecise knowledge of the PDF's introduces an additional 5.7% uncertainty on signal acceptance.

## IV. RESULTS

The observed number of events  $N_{obs}^{ev} = 487$  is in agreement with  $N_{bg}^{ev}$ , indicating that there is no significant excess of events from non-SM processes. The uncertainties in background estimation are comparable to, or larger than the expected signal for a wide range of MSSM scenarios.

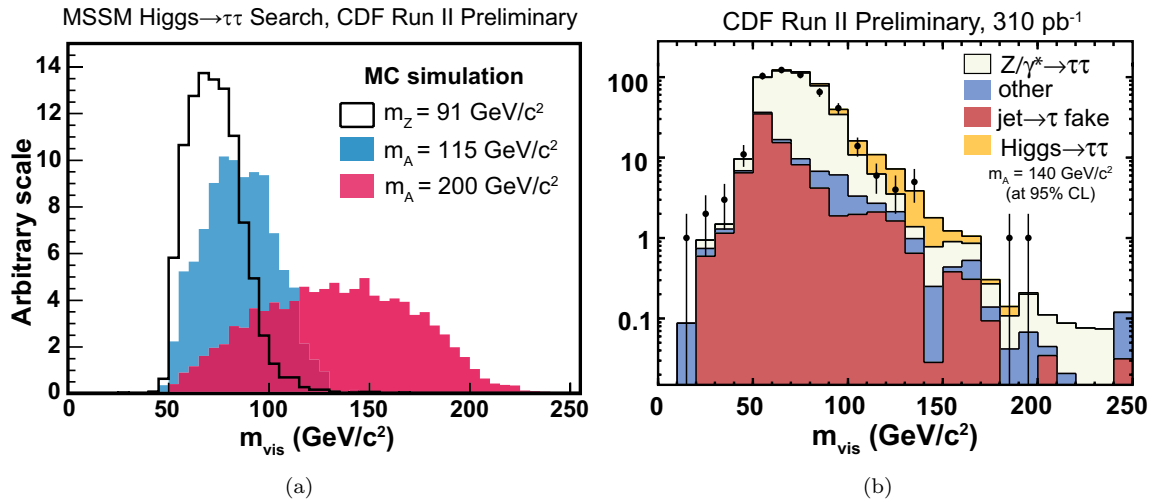


FIG. 2: Distribution of  $m_{vis}$  for  $Z \rightarrow \tau\tau$  and  $m_A = 115, 200$  GeV/c<sup>2</sup> for MC simulated events (a). Backgrounds and signal with  $m_A = 140$  GeV/c<sup>2</sup> in logarithmic scale - the normalization corresponds to the fit results for signal exclusion at 95% CL (b).

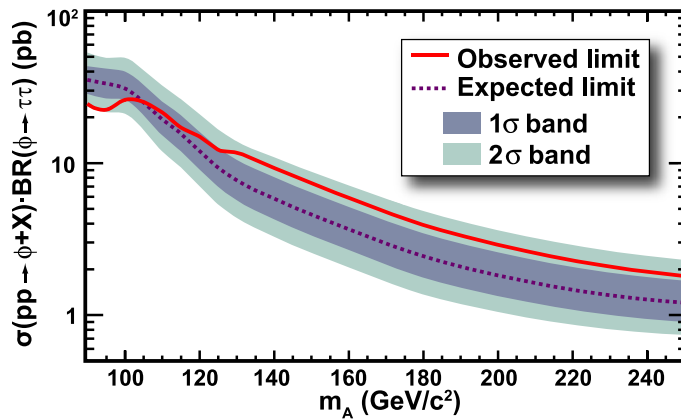


FIG. 3: Observed and expected limits at 95% CL for Higgs production cross-section times branching fraction to  $\tau$  pairs.

To probe for possible Higgs signal we perform binned likelihood fits of the partially reconstructed mass of the di- $\tau$  system ( $m_{vis}$ ) defined as the invariant mass of the visible tau decay products and  $\cancel{E}_T$ . The MC predictions for the  $m_{vis}$  shapes for the irreducible background and two signal points are shown in Figure 2a. In the fits, the backgrounds are allowed to float within limits set by Gaussian constraints corresponding to the systematic uncertainties in trigger efficiencies, particle identification, production cross sections, PDF's, event cuts, and luminosity measurement. Potential differences in  $m_{vis}$  shapes between data and the MC simulation in different channels are treated as systematic uncertainties. We create signal and background  $m_{vis}$  templates with the MC energy scales shifted from the nominal values according to the uncertainties, and study the effect on hypothetical cross section measurements. The deviations from the results obtained with the nominal templates are parameterized in terms of Higgs mass and input cross section. An example fit for  $m_A = 140$  GeV/c<sup>2</sup> is shown in Figure 2b.

We observe no signal evidence for  $m_A = 90 - 250$  GeV/c<sup>2</sup>, and set exclusion limits at 95% CL on  $\sigma(pp \rightarrow \phi + X) \times BR(\phi \rightarrow \tau\tau)$  as shown in Figure 3. The sensitivity of the limit-setting procedure is determined from MC simulations assuming no signal. The  $m_{vis}$  shape uncertainty leads to 15% (5%) deterioration of the limits for the low

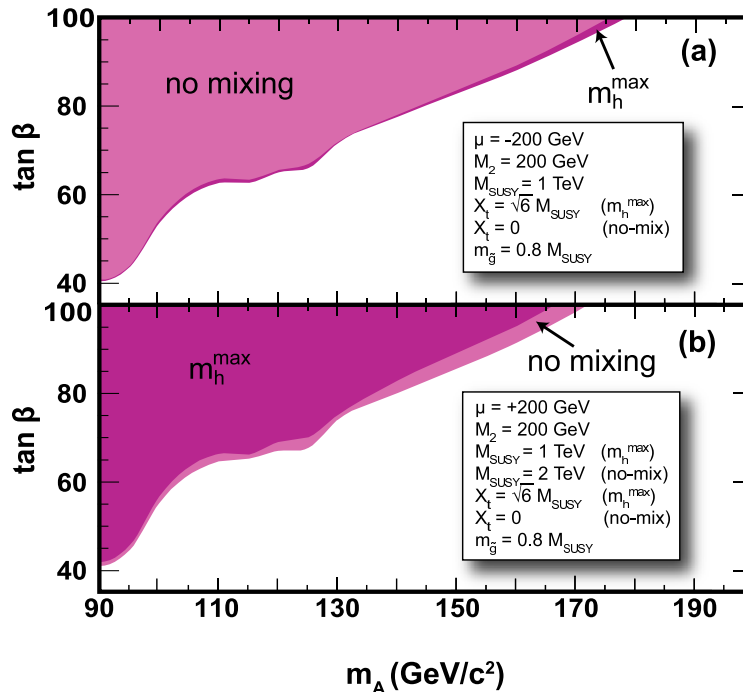


FIG. 4: Excluded region in  $\tan\beta$  vs  $m_A$  plane for the  $m_h^{max}$  and no-mixing scenarios with  $\mu < 0$  (a), and  $\mu > 0$  (b).

(high) end of the considered  $m_A$  region.

## V. INTERPRETATION OF THE RESULTS IN MSSM

Using the theoretical predictions for the MSSM Higgs production and decay to  $\tau$  pairs we interpret the limits on  $\sigma(pp \rightarrow \phi + X) \times BR(\phi \rightarrow \tau\tau)$  as exclusions of parameter regions in the  $\tan\beta$  vs  $m_A$  plane. The cross sections are obtained from SM calculations and scaling factors  $\sigma_{MSSM}/\sigma_{SM}$  accounting for the modified Higgs couplings [13]. The cross sections for gluon fusion mediated by a  $b$ -quark loop are calculated with the HIGLU program [14]. The corresponding values for  $b\bar{b} \rightarrow \phi + X$  are taken from [4]. The scaling factors and  $BR(\phi \rightarrow \tau\tau)$  are calculated with the FeynHiggs program [15]. They depend on  $m_A$ ,  $\tan\beta$ , the  $SU(2)$  gaugino mass parameter  $M_2$ , the SUSY mass scale  $M_{SUSY}$ , the squark mixing parameter  $X_t$ , the gluino mass  $m_{\tilde{g}}$ , and the Higgs mixing parameter  $\mu$ . We consider four benchmarks [16]: the  $m_h^{max}$  and no-mixing scenarios, with  $\mu > 0$  and  $\mu < 0$ . The excluded  $\tan\beta$  regions as a function of  $m_A$  are shown in Figure 4.

## VI. CONCLUSION

The di- $\tau$  decay channel is a powerful search mode for neutral MSSM Higgs bosons produced in  $p\bar{p}$  collisions. The LEP experiments have excluded  $m_A \lesssim 93$  GeV/c<sup>2</sup>, and higher-mass  $A$  for small  $\tan\beta$  [17]. Our search is complementary, providing sensitivity in the large  $\tan\beta$  region. The excluded parameter space in the  $\tan\beta$  vs  $m_A$  plane for  $\mu < 0$  is similar to the  $D\bar{O}$  results obtained in the  $\phi \rightarrow b\bar{b}$  decay mode [18], and extends to higher  $m_A$ . Moreover, our results in the  $\phi \rightarrow \tau\tau$  channel allow us to set comparable exclusions for scenarios with  $\mu > 0$ , as the lower production cross sections are compensated by an increase in  $BR(\phi \rightarrow \tau\tau)$ . The present search is statistics limited and the sensitivity will increase with the addition of the  $\tau_e\tau_\mu$  and  $\tau_{had}\tau_{had}$  final states and more data.

### Acknowledgments

We would like to thank A. Belyaev, M. Carena, J. Gunion, S. Heinemeyer, W. Kilgore, S. Mrenna, M. Spira, C. Wagner, G. Weiglein, and S. Willenbrock for illuminating discussions on the theory of MSSM Higgs production and decays.

We thank the Fermilab staff and the technical staffs of the participating institutions for their vital contributions. This work was supported by the U.S. Department of Energy and National Science Foundation; the Italian Istituto Nazionale di Fisica Nucleare; the Ministry of Education, Culture, Sports, Science and Technology of Japan; the Natural Sciences and Engineering Research Council of Canada; the National Science Council of the Republic of China; the Swiss National Science Foundation; the A.P. Sloan Foundation; the Bundesministerium für Bildung und Forschung, Germany; the Korean Science and Engineering Foundation and the Korean Research Foundation; the Particle Physics and Astronomy Research Council and the Royal Society, UK; the Russian Foundation for Basic Research; the Comisión Interministerial de Ciencia y Tecnología, Spain; in part by the European Community's Human Potential Programme under contract HPRN-CT-2002-00292; and the Academy of Finland.

- 
- [1] P.W. Higgs, Phys. Lett. **12**, 132 (1964), Phys. Rev. Lett. **13**, 508 (1964), Phys. Rev. **145**, 1156 (1966).
  - [2] S. Dawson, A. Djouadi, and M. Spira, Phys. Rev. Lett. **77**, 16 (1996).
  - [3] F. Maltoni, Z.Sullivan, and S. Willenbrock, Phys. Rev. **D67**, 093005 (2003).
  - [4] R.V. Harlander, W.B. Kilgore, Phys. Rev. **D68**, 013001 (2003).
  - [5] S. Klimentenko, J. Konigsberg, and T.M. Liss, FERMILAB-FN-0741 (2003).
  - [6] D. Acosta *et al.*, Phys. Rev. **D71**, 032001 (2005).
  - [7] A. Anastassov *et al.*, Nucl. Instrum. and Methods **A518**, 609 (2004).
  - [8] T. Sjöstrand *et al.*, Comput. Phys. Commun. **135**, 238 (2001). We use PYTHIA v. 6.215.
  - [9] H.L. Lai *et al.* (CTEQ Collaboration), Eur. Phys. J. C **12**, 375 (2000).
  - [10] Z. Was *et al.*, Nucl. Phys. Proc. Suppl. **98**, 96 (2001).
  - [11] R. Brun and F. Carminati, CERN Programming Library Long Writeup **W5013** (1993).
  - [12] D. Acosta *et al.* (CDF Collaboration), Phys. Rev. Lett. **94**, 091803 (2005).
  - [13] M. Carena, S. Heinemeyer, G. Weiglein, and C.E.M. Wagner, FERMILAB-PUB-05-370-T (2005).
  - [14] M. Spira, Nucl. Instrum. Meth. **A389**, 357 (1997).
  - [15] S. Heinemeyer, W. Hollik, and G. Weiglein, Eur. Phys. J. C **9**, 343 (1999); Comput. Phys. Commun. **124**, 76 (2000).
  - [16] M. Carena, S. Heinemeyer, C.E.M. Wagner, and G. Weiglein, hep-ph/9912223 (1999); Eur. Phys. J. C **26**, 601 (2003).
  - [17] ALEPH, DELPHI, L3, and OPAL Collaborations, LHWG-Note 2004-01 (2004).
  - [18] V. Abazov *et al.* (DØ Collaboration), hep-ex/0504018 (2005).